J Solution Chem (2017) 46:1024–1047
DOI 10.1007/s10953-017-0621-z

Potentiometric and Speciation Studies on the Complex Formation Reactions of [Pd(2-methylaminomethyl)-pyridine)$(H_2O)_2]^{2+}$ with Some Bio-active Ligands and Displacement Reaction of Coordinated Inosine

Abeer T. Abd El-Karim[1] · Islam R. El-Sherif[1] · Wafaa M. Hosny[1] · Eyad K. Alkhadhairi[2] · Mutlaq S. Aljahdali[3] · Ahmed A. El-Sherif[1,4]

Received: 19 November 2016 / Accepted: 13 March 2017 / Published online: 10 May 2017

Abstract The stoichiometry and stability constants of the complexes formed between $[Pd(MAMP)(H_2O)_2]^{2+}$ and various biologically relevant ligands containing different functional groups were investigated. The ligands used are amino acids, peptides and DNA constituents. The results show the formation of 1:1 complexes with amino acids and peptides and the corresponding deprotonated amide species. Structural effects of peptides on amide deprotonation were investigated. The purine and pyrimidine bases uracil, uridine, cytosine, inosine, inosine 5′-monophosphate (5′-IMP) and thymine form 1:1 and 1:2 complexes. The concentration distribution of the various complex species was calculated as a function of pH. The effect of chloride ion concentration on the formation constant of CBDCA with $Pd(MAMP)^{2+}$ was also reported. The results show ring opening of CBDCA and monodentate complexation of the DNA constituent with the formation of [Pd(MAMP)(CBDCA-O)DNA], where (CBDCA-O) represents cyclobutane dicarboxylate coordinated by one carboxylate oxygen. The equilibrium constant of the displacement reaction of coordinated inosine, as a typical DNA constituent, by SMC and/or methionine was calculated. The results are expected to contribute to the chemistry of antitumor agents. The calculated parameters of the optimized complexes support the measured formation constants.

Electronic supplementary material The online version of this article (doi:10.1007/s10953-017-0621-z) contains supplementary material, which is available to authorized users.

✉ Abeer T. Abd El-Karim
tabdelkarim@yahoo.com

✉ Ahmed A. El-Sherif
aelsherif72@yahoo.com

[1] Faculty of Science, Chemistry Department, Cairo University, Giza, Egypt

[2] Faculty of Pharmacy, Northern Border University, Rafha, Saudi Arabia

[3] Faculty of Science, Chemistry Department, King AbdAl-Aziz University, Jeddah, Saudi Arabia

[4] Faculty of Arts and Science, Chemistry Department, Northern Border University, Rafha, Saudi Arabia

Keywords 2-(Methylamino)methylpyridine · Amino acids · Peptides · DNA constituents · Potentiometric titration

Abbreviations

CBDCA	1,1-Cyclobutanedicarboxylic acid
MAMP	2-(Methylamino)methylpyridine
5′-IMP	Inosine-5′-monophosphate
5′-GMP	Guanosine-5′-monophosphate
SMC	S-methyl-L-cysteine
DMEN	*N*,*N*′-Dimethylethylenediamine
Thr	Threonine
Ser	Serine
En	Ethylenediamine
1,3-DAP	1,3-Diaminopropane
BPY	*N*,*N*′-Bipyridyl
α-Ala	α-Alanine
β-Ala	β-Alanine
PM3	Parametric Method-3
UV	Ultraviolet
HOMO	Highest occupied molecular orbital energy
LUMO	Lowest unoccupied molecular orbital energy
χ	Mulliken electronegativity
Pi	Chemical potential
η	Global hardness
S	Global softness
ω	Global electrophilicity

1 Introduction

Since the discovery of the antitumor properties of platinum compounds by Rosenberg et al. [1], cisplatin has demonstrated a remarkable chemotherapeutic potential in a large variety of human solid cancers, including testicular, ovarian, bladder, lung and stomach carcinomas [2, 3]. A large number of analogs have been tested. The replacement of ammonia by other amines such as cyclopentylamine and cyclohexylamine has sresulted in higher therapeutic indices than cisplatin and some of these are potential second-generation drugs [4, 5]. Cisplatin and other second-generation platinum drugs have draw-backs such as high nephorotoxicity, low water solubility and relative inactivity against gastrointestinal tumors [6]. Furthermore, the development of an acquired resistance to cisplatin is frequently observed during chemotherapy [7]. In recent years, work from our groups and others has concentrated on the reactions of Pt^{II} and Pd^{II} complexes with nitrogen containing biomolecules [8–21], which could be of fundamental importance in the understanding of the mechanism of antitumor activity of related platinum complexes. For mechanistic studies of the action of Pt^{II} antitumor drugs, their Pd^{II} analogues are usually good model compounds since they exhibit a 10^4–10^5 fold higher reactivity, whereas coordination geometry and complex formation processes of palladium(II) are very similar to those of platinum(II); thus palladium(II) ions are frequently used to mimic the binding properties of various platinum(II) species [22]. On this basis Gill [6] has reported several palladium complexes

with bidentate amine ligands that have shown anticancer activity comparable to or greater than cisplatin. Much work has been carried out on the equilibrium studies of palladium(II) complexes with aliphatic amines [23–25] and it is of considerable interest to extend this work to other palladium complexes with aromatic heterocycles such as 2-(methylamino)methylpyridine. The aromatic heterocycles act as σ-donors and can also function as fairly effective π-acceptors. The π-accepting properties can be involved in π–π stacking effects with purine and pyrimidine bases. This will enhance complex formation with DNA subunits, which is the principal target in the chemotherapy of tumors. As part of our interest in the synthesis, structure and reactivity of coordination complexes of Pd^{II} with chelating ligands [23–26], and with the aim of extending our earlier work in this area, we report here a detailed study on the complex formation equilibrium of $[Pd(MAMP)(H_2O)_2]^{2+}$ with biologically relevant ligands. The effect of chloride ion concentration on the formation of Pd(MAMP)–CBDCA (as a representative example), is also investigated.

2 Experimental

2.1 Materials

All chemicals used were of the analytical reagent grade (AR) and of highest purity. Ligand stock solutions were prepared shortly before use by dissolving the chemicals in deionized water. Amino acids, peptides and DNA constituents investigated are: glycine (Gly, Aldrich, assay ≥ 99.0%), alanine (Ala, Aldrich, assay ≥ 98.0%), β-alanine (β-Ala, Aldrich, assay = 99.0%), valine (Val, Aldrich, assay ≥ 98.0%), proline (Pro, Aldrich, assay ≥ 99.0%), threonine (Thr, Aldrich, assay ≥ 98.0%), serine (Ser, Aldrich, assay ≥ 99.0%), S-methylcysteine (SMC, Aldrich, assay ≥ 98.0%), ornithine (Orn, Aldrich, assay ≥ 99.0%), L-methionine (Met, Fluka, assay > 99.0%), glycinamide (GA, Aldrich, assay = 99.0%), glycylglycine (GlyGly, Aldrich, assay ≥ 99.0%), glutamine (Glu, Aldrich, assay ≥ 99.0%), glycylalanine (GlyAla, Aldrich, assay ≥ 99.0%), uracil (Aldrich, assay ≥ 99.0%), uridine (Aldrich, assay ≥ 99.0%), thymine (Aldrich, assay ≥ 99.0%), cytosine (Aldrich, assay ≥ 99.0%), inosine (Aldrich, assay ≥ 99.0%) and inosine 5′-monophosphate (Aldrich, assay ≥ 99.0%). Additionally, 1,1-cyclobutanedicarboxylic acid ($CBDCAH_2$, Aldrich, assay = 99.0%) was provided also by Aldrich Chemical Company. These materials were provided by Sigma Chemicals Company and used without further purification. Also, methylamine hydrochloride (Aldrich, assay > 98.0%) and imidazole (Aldrich, assay > 98.0%) were provided by Sigma Chemicals Company. Carbonate-free NaOH (titrant) was prepared and standardized against potassium hydrogen phthalate solution daily. All solutions were prepared in deionized H_2O.

2.2 Preparation of the Diaqua $[Pd(MAMP)(H_2O)_2](NO_3)_2$ Complex

In this study, $[Pd(MAMP)Cl_2]$ was prepared by heating $PdCl_2$ (532.2 mg, 3 mmol) in 50 mL water and KCl (447 mg, 6 mmol) to 50 °C for 30 min. After the $K_2[PdCl_4]$ solution cooled, 2-(methylamino)methyl pyridine (366.51 mg, 3 mmol), dissolved in 10 mL water, was added dropwise with stirring. A yellow precipitate formed, and the mixture was stirred for a further 1 h at 25 °C. After the precipitate was filtered off, it was washed sequentially with water, ethanol and diethyl ether.

The diaqua-complex $[Pd(MAMP)(H_2O)_2](NO_3)_2$ was prepared in solution by stirring the chloro complex with two equivalents of $AgNO_3$ overnight, and removing the AgCl precipitate by filtration through a 0.1 μm pore membrane filter. Great care was taken to ensure that the resulting solution was free of Ag^+ ions and that the chloro complex had been converted into the aqua species. The filtrate was made up to the desired volume in a standard volumetric flask. The ligands in the form of hydrochlorides were converted to the corresponding hydronitrate in the same way as described above.

2.3 Apparatus

Potentiometric measurements were made using a Metrohm 686 titroprocessor equipped with a 665 Dosimat (Switzerland-Herisau). The thermostatted glass cell was equipped with a magnetic stirring system, a Metrohm glass-calomel combined electrode, a thermometric probe and a microburet delivery tube. The titroprocessor and electrode were calibrated daily with standard buffer solutions prepared according to NBS specifications at 25.0 ± 0.1 °C [27] and $I = 0.1$ mol·dm^{-3}, potassium hydrogen phthalate (pH = 4.008) and a mixture of KH_2PO_4 and Na_2HPO_4 (pH = 6.865).

2.4 Procedure and Measuring Techniques

The acid dissociation constants of the ligands were determined potentiometrically by titrating 40 cm^3 of ligand solution (1.25×10^{-3} mol·dm^{-3}). The acid-dissociation constants of the coordinated water molecules in $[Pd(MAMP)(H_2O)_2)]^{2+}$ were determined by titrating a 1.25×10^{-3} mol·dm^{-3} solution of the complex. The formation constants of the complexes were determined by titrating solution mixtures of $[Pd(MAMP)(H_2O)_2]^{2+}$ (1.25×10^{-3} mol·dm^{-3}) and the ligand in concentration ratios of 1:1 for amino acids and peptides, and for concentration ratios of 1:1 and 1:2 (metal:ligand) for DNA constituents. The titration solution mixtures had a volume of 40 mL. Temperature was maintained constant inside the cell at (25.0 ± 0.1) °C, by circulating thermostated water through the double-wall of the titration vessel and titrations were performed with a slow and constant stream of N_2 over the test solutions. The pH meter readings were converted into hydrogen ion concentrations by titrating a standard acid solution (0.05 mol·dm^{-3}), the ionic strength of which was adjusted to 0.1 mol·dm^{-3}, with standard base solution (0.05 mol·dm^{-3}) at 25 °C. The pH was plotted against p[H]. The relationship pH – p[H] = 0.05 was observed. The [OH$^-$] values were calculated using a pK_w value of 13.997 [28]. The ionic strength was adjusted to 0.1 mol·dm^{-3} using $NaNO_3$. The equilibrium constants evaluated from the titration data (defined by Eqs. 1 and 2) are:

$$lM + pL_1 + qL_2 + rH \overset{\beta_{lpqr}}{\rightleftharpoons} M_lL_{1p}L_{2q}H_r \tag{1}$$

$$\beta_{lpqr} = \frac{[M_lL_{1p}L_{2q}H_r]}{[M]^l[L_1]^p[L_2]^q[H]^r} \tag{2}$$

where M, L and H stand for the $[Pd(MAMP)(H_2O)_2]^{2+}$ ion, ligand and proton, respectively. The calculations were carried out using ca. 100 data points in each titration, using the computer program MINIQUAD-75 [29]. The stoichiometry and stability constants of the complexes formed were determined by trying various possible composition models. The model selected gave the best statistical fit and was chemically consistent with the titration data without giving any systematic drifts in the magnitudes of various residuals, as

described elsewhere [29]. The fitted model was tested by comparing the experimental titration data points and the theoretical curve calculated from the values of the acid dissociation constant of the ligand and the formation constants of the corresponding complexes. The species distribution diagrams were obtained using the program SPECIES [30] under the experimental conditions employed.

2.5 Molecular modeling studies

An attempt to gain a better insight on the molecular structure of the compounds, geometry optimization and conformation analysis was performed using the semi-empirical method PM3 as implemented in HyperChem 7.5 [31]. A gradient of 0.04 kJ·Å^{-1} was set as a convergence criterion in all the molecular mechanics and quantum calculations. The lowest energy structure was used for each molecule to calculate physicochemical properties.

2.6 Spectrophotometric Measurements

Spectrophotometric measurements of the Pd(MAMP)–glycyinamide complex were performed by recording the UV–visible spectra of solutions (A–C) as follows:

(A) 0.001 mol·dm^{-3} $[Pd(MAMP)(H_2O)_2]^{2+}$;
(B) 0.001 mol·dm^{-3} $[Pd(MAMP)(H_2O)_2]^{2+}$ + 0.001 mol·dm^{-3} glycyinamide + 0.001 mol·dm^{-3} of NaOH
(C) 0.001 mol·dm^{-3} of $[Pd(MAMP)(H_2O)_2]^{2+}$ + 0.001 mol·dm^{-3} glycyinamide + 0.002 mol·dm^{-3} NaOH.

Under these experimental conditions, and after neutralization of the hydrogen ions released associated with complex formation, it is supposed that the complexes have been completely formed. In each mixture, the volume was brought to 10 mL by addition of deionized water and ionic strength was kept constant at 0.1 mol·dm^{-3} with $NaNO_3$.

3 Results and Discussion

The acid dissociation constants of the ligands were determined under the experimental conditions of (25 ± 0.1) °C and a constant ionic strength of 0.1 mol·dm^{-3}, which were also used to determine the stability constants of the $Pd^{(II)}$ complexes. The values obtained are consistent with data reported in the literature [32].

3.1 Hydrolysis of $[Pd(MAMP)(H_2O)_2]^{2+}$

The hydrolysis of the $[Pd(MAMP)(H_2O)_2]^{2+}$ complex was studied by fitting the potentiometric data to various models. The best fit model was found to be consistent with the species 10–1, 10–2 and 20–1, as given in Eqs. 3–5:

$$\underset{100}{\left[Pd(MAMP)(H_2O)_2\right]^{2+}} \rightleftharpoons \underset{10-1}{[Pd(MAMP)(H_2O)(OH)]^{+}} + H^{+} \quad (3)$$

$$\underset{10-1}{[Pd(MAMP)(H_2O)(OH)]^{+}} \rightleftharpoons \underset{10-2}{\left[Pd(MAMP)(OH)_2\right]^{0}} + H^{+} \quad (4)$$

$$\underset{100}{\left[\mathrm{Pd(MAMP)(H_2O)_2}\right]^{2+}} + \underset{10-1}{\left[\mathrm{Pd(MAMP)(H_2O)(OH)}\right]^{+}} \rightleftharpoons \underset{20-1}{\left[\left(\mathrm{Pd(MAMP)(H_2O)_2}\right)_2\mathrm{(OH)}\right]^{3+}} + \mathrm{H_2O} \quad (5)$$

The first two species are due to deprotonation of the two coordinated water molecules, as given by Eqs. 3 and 4, and the negative numbers refer to proton loss. The hydroxo bridged-dimer (20–1) with a single hydroxyl bridge may be formed as result of the combination of the monoaqua hydroxo species (10–1) with the diaqua species (100) $[Pd(MAMP)(H_2O)_2]^{2+}$ as given by Eq. 5.

The pK_{a1} and pK_{a2} values were found to be 4.69 and 10.08, respectively. The pK_{a1} value is lower than that for $[Pd(1,3\text{-}DAP)(H_2O)_2]^{2+}$($pK_a = 5.96$) [21]. This shows that the first coordinated water molecule in $[Pd(MAMP)(H_2O)_2]^{2+}$ is more acidic than that of $[Pd(en)(H_2O)_2]^{2+}$, which may be attributed to the π-acceptor properties of the aromatic moiety of MAMP, leading to an increase in the electrophilicity of the Pd ion and a consequent decrease of the pK_a of the coordinated water molecule. The pK_{a1} (4.69) of $[Pd(MAMP)(H_2O)_2]^{2+}$ is higher than that of $[Pd(BPY)(H_2O)_2]^{2+}$ (3.81) and pK_{a2} (10.08) is higher also than that of $[Pd(BPY)(H_2O)_2]^{2+}$ (8.39) [33], this may be due to the presence of the two aromatic moieties in bipyridyl, which increases the the π-acceptor properties and the electrophilicity of the Pd ion more than presence of the one aromatic ring in the case of 2-(methylamino)methylpyridine. The μ-hydroxo species (20–1) is assumed to form through dimerization of the $Pd^{(II)}$ complex via a hydroxo group.

The equilibrium constant for the dimerization reaction (Eq. 5) can be calculated by Eq. 6 from the formation constants listed in Table 1, and amounts to $\log_{10} K_d = 3.95$.

$$\log_{10} K_d = \log_{10} \beta_{20-1} - \log_{10} \beta_{10-1}. \quad (6)$$

The distribution diagram for $[Pd(MAMP)(H_2O)_2]^{2+}$ and its hydrolyzed form reveals that the concentration of the monohydroxo species (10–1) and the μ-hydroxo species (20–1) increase with increasing pH. The monohydroxo (10–1) complex reaches its maximum concentration of 98% at pH = 7.8 while the μ-hydroxo species (20–1) reaches its maximum concentration of 66% at pH = 4.6, i.e., they are approximately the main species present in solution in the physiological pH range. A further increase in pH is accompanied by an increase in the concentration of dihydroxo species, which is the main species above a pH of ca. 11, i.e., in the high pH range the inert dihydroxo complex would be the predominant species, so that the reactivity of DNA to bind the Pd(amine) complex will considerably decrease.

3.2 Amino Acid Complexes

Analysis of pH titration data for Pd(MAMP)–amino acid systems showed the formation of 1:1 complexes with stability constants larger than for the corresponding monodentate methylamine and imidazole complexes. This indicates that amino acids bind through the amino and carboxylate groups as given in Scheme 1.

Comparison of the stability constant of the α-alanine (11.42) and β-alanine (8.79) complexes indicates that the five-membered chelate ring formed in the α-alanine complex is the most favored, whereas the six-membered chelate ring formed in the β-alanine amino acid complex is least favored as given in Scheme 2.

Serine and threonine have an extra binding center on the β-alcoholate group. This group was reported [34, 35] to participate in transition metal ion complex formation reactions. The pK_a values of the β-alcoholate group incorporated in the Pd(II) complex ($\log_{10} \beta_{110}$ –

Table 1 Protonation constants of some selected amino acids and their formation constants with $[Pd(MAMP)(H_2O)_2]^{2+}$ at 25 °C and 0.1 mol·dm^{-3} ionic strength

Ligand	l	p	r[a]	$\log_{10}\beta$[b]	S[c]
OH^-	1	0	−1	−4.69 (0.05)	6.71×10^{-7}
	1	0	−2	−14.77 (0.07)	
	2	0	−1	−0.74 (0.09)	
Glycine	0	1	1	9.60 (0.01)	1.50×10^{-7}
	0	1	2	11.93 (0.03)	
	1	1	0	10.30 (0.07)	3.53×10^{-7}
Alanine	0	1	1	9.69 (0.01)	9.21×10^{-8}
	0	1	2	11.88 (0.02)	
	1	1	0	11.42 (0.05)	6.70×10^{-8}
β-alanine	0	1	1	9.12 (0.01)	3.5×10^{-7}
	0	1	2	11.39 (0.02)	
	1	1	0	8.79 (0.05)	3.73×10^{-7}
Valine	0	1	1	9.57 (0.01)	9.90×10^{-8}
	0	1	2	11.70 (0.03)	
	1	1	0	10.55 (0.1)	2.85×10^{-6}
Proline	0	1	1	10.52 (0.01)	4.42×10^{-8}
	0	1	2	12.03 (0.03)	
	1	1	0	12.42 (0.08)	7.61×10^{-7}
Threonine	0	1	1	9.06 (0.01)	7.93×10^{-8}
	0	1	2	11.03 (0.02)	
	1	1	0	10.77 (0.08)	3.20×10^{-7}
	1	1	−1	2.90 (0.09)	
Serine	0	1	1	9.14 (0.01)	1.72×10^{-8}
	0	1	2	11.40 (0.01)	
	1	1	0	11.27 (0.09)	3.75×10^{-7}
	1	1	−1	3.31 (0.09)	
Methionine	0	1	1	9.10 (0.01)	8.91×10^{-8}
	0	1	2	11.08 (0.03)	
	1	1	0	9.42 (0.05)	4.07×10^{-7}
S-methylcysteine	0	1	1	8.51 (0.01)	3.44×10^{-8}
	0	1	2	10.52 (0.03)	
	1	1	0	9.63 (0.07)	2.11×10^{-6}
Orinthine	0	1	1	10.58 (0.00)	1.03×10^{-8}
	0	1	2	19.43 (0.02)	
	0	1	3	21.39 (0.02)	
	1	1	0	11.95 (0.05)	1.02×10^{-7}
	1	1	1	20.44 (0.05)	
Methylamine	0	1	1	10.03 (0.04)	4.40×10^{-7}
	1	1	0	7.32 (0.03)	1.81×10^{-7}
	1	2	0	13.45 (0.05)	

Table 1 continued

Ligand	*l*	*p*	*r*[a]	$\log_{10} \beta$[b]	S[c]
Imidazole	0	1	1	7.04 (0.01)	3.15×10^{-8}
	1	1	0	7.01 (0.04)	5.01×10^{-7}
	1	2	0	10.29 (0.07)	

[a] *l*, *p* and *r* are the stoichiometric coefficients corresponding to $Pd(MAMP)^{2+}$, amino acid, and H^+, respectively

[b] Standard deviations are given in parentheses

[c] Sum of square of residuals

Scheme 1 Coordination modes of imidazole as monodentate ligand and glycine as bidentate ligand with $[Pd(MAMP)(H_2O)_2]^{2+}$ complex

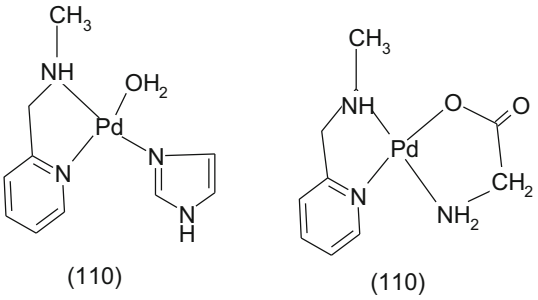

Scheme 2 Structural formulae of [Pd(MAMP)-α-Ala] and [Pd(MAMP)-β-Ala] complexes

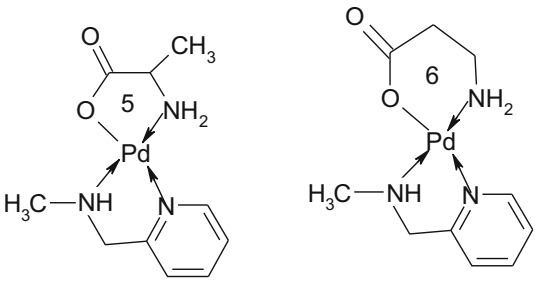

$\log_{10} \beta_{11-1}$) for threonine and serine amino acid complexes are 7.87 and 7.96, respectively (Table 1), i.e., the alcohol group of serine is competing with the carboxylate group in binding to the $Pd(MAMP)^{2+}$ ion. Due to the donation of the electron pair on the oxygen to the metal center, the OH bond is considerably weakened and thus the ionization of the proton occurs at a lower pH with respect to the higher pK_a value ($pK_a = \sim 14$) of the hydroxo group of the free serine and threonine amino acids. These values are lower than that of the Pd(N,Ń-dimethylethylenediamine)–serine complex (8.43) [23]. This may be explained on the premise that the presence of the aromatic moiety in 2-(methylamino)methylpyridine increases the electrophilic character of the Pd(II) ion and hence the pK_a value of the coordinated alcoholate group decreases.

The pK_a values of the alcoholate group incorporated in [Pd(SMC)Ser] and [Pd(SMC)Thr] (where SMC = S-methyl-L-cysteine), are 9.26 and 9.29 (Table 1S) for serine and threonine, respectively, as reported in literature [36]. These pK_a values reported in the literature [36] for the [Pd(SMC)Ser] and [Pd(SMC)Thr] complexes are higher than the corresponding values of the [Pd(MAMP)Ser] (pK_a = 7.96) and [Pd(MAMP)Thr] (pK_a = 7.87) complexes, i.e., the pK_a value in case of the S-methyl-L-cysteine complex is higher than that of the dinitrogen complex. This is due to the strong trans labilization effect of sulfur on the coordinated alcoholate group, which weakens the bond between the S atom and the alcohol group and in turn hinders the induced proton ionization causing an in increase the pK_a value of the alcoholate group in the case of the Pd(SMC)–serine complex. The distribution diagram for the threonine complex is given in Fig. 1S. The complex species with coefficients 110 reaches its maximum degree of formation (98%) at pH = 4.4–6.6, i.e., in the physiological pH range. However, the species 11−1 attains a maximum concentration of 97% at pH ca. 10.4.

S-methylcysteine forms a more stable complex than the methionine amino acid, plausibly due to the fact that the five-membered chelate ring in the former complex is energetically favored over the six-membered chelate ring in the latter complex.

Ornithine has one carboxylic and two amino groups. It coordinates as a bidentate ligand using either a (N,N) or (N,O) donor set. The stability constant of its complex is higher than those of α-amino acids (N,O donor sets). This may be taken as an indication that ornithine chelates using the (N,N) donor set. This formulation is supported by the high affinity of Pd(II) to nitrogen donor centers. Ornithine forms, in addition to 1:1 complexes, the monoprotonated 111 complex species. The pK_a of the protonated complex was calculated from Eq. 7:

$$pK_a = \log_{10}\beta_{111} - \log_{10}\beta_{110} \tag{7}$$

The pK_a value of the protonated species is 8.49 for ornithine.

The species distribution for ornithine complex, taken as representative, is given in Fig. 2S. The protonated species 111 complex predominates (95% at pH ca. 5.6); the deprotonated species 110 complex predominates (94% at pH ca. 10.2); the hydroxo complex $[Pd(MAMP)(H_2O)(OH)]^+$ plays a minor role in that region. This means that in the physiological pH range the OH^- ion does not compete with the amino acid in the reaction with the $[Pd(MAMP)(H_2O)_2]^{2+}$ complex.

3.3 Complex Formation Equilibria Involving Peptides

The potentiometric data for the Pd(MAMP)–peptide system were fitted to various models. The most acceptable model, as given in Scheme 3, was found to be consistent with the formation of complexes with stoichiometric coefficients 110 and 11–1.

In the 110 species, the peptide is bound through the amino and carbonyl groups. Upon deprotonation of the amide group, the coordination sites could switch from the carbonyl oxygen to the amide nitrogen such that the 11–1 complex is formed. Such changes in coordination modes are well documented [37]. The glutamine complex ($\log_{10}\beta_{110}$ = 9.73) is more stable than the glycinamide complex ($\log_{10}\beta_{110}$ = 8.11), presumably due to the fact that glutamine carries a negative charge whereas glycinamide is neutral. The electrostatic interaction between the glutaminate and the positively charged Pd(II) complex will result in a lowering of the Gibbs energy of formation. The pK_a values of the amide group, incorporated in the Pd(II) complex ($\log_{10}\beta_{110} - \log_{10}\beta_{11-1}$), are in the range

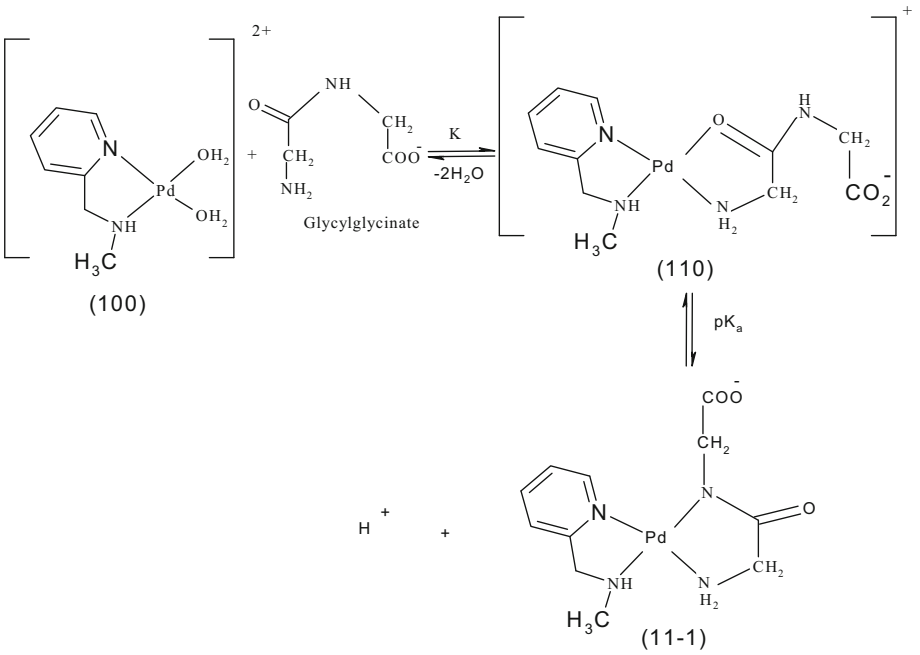

Scheme 3 Coordination modes of GlyGly with the $[Pd(MAMP)(H_2O)_2]$ complex

Table 2 Protonation constants of some selected peptides and their formation constants with $[Pd(MAMP)(H_2O)_2]^{2+}$ at 25 °C and 0.1 mol·dm^{-3} ionic strength

System	*l*	*p*	*r*[a]	$\log_{10}\beta$[b]	pK_a	S[c]
Glycinamide	0	1	1	7.68 (0.00)	4.59	4.51×10^{-8}
	1	1	0	8.11 (0.02)		
	1	1	−1	3.52 (0.04)		1.72×10^{-7}
Glycylglycine	0	1	1	7.98 (0.01)	8.04	4.03×10^{-8}
	1	1	0	8.31 (0.02)		1.01×10^{-7}
	1	1	−1	0.27 (0.03)		
Glutamine	0	1	1	8.92 (0.00)	9.44	3.04×10^{-8}
	1	1	0	9.73 (0.06)		1.62×10^{-7}
	1	1	−1	0.29 (0.08)		
Glycylalanine	0	1	1	8.04 (0.00)	5.38	4.41×10^{-8}
	1	1	0	8.46 (0.05)		9.15×10^{-7}
	1	1	−1	3.08 (0.06)		

[a] *l*, *p* and *r* are the stoichiometric coefficients corresponding to $Pd(MAMP)^{2+}$, peptide and H^+, respectively

[b] Standard deviations are given in parentheses

[c] Sum of square of residuals

4.59–9.44 (Table 2). The low pK_a values in the present study are probably due to the high affinity of Pd(II) for nitrogen donor ligands. It is interesting to note that the pK_a value for the glycinamide complex is lower than those for other peptides. This can be explained on the basis that the more bulky substituent on the peptide may hinder structural changes when going from the protonated to the deprotonated complexes. The pK_a of the glutamine complex is exceptionally higher than those for the other peptide complexes. This is due to

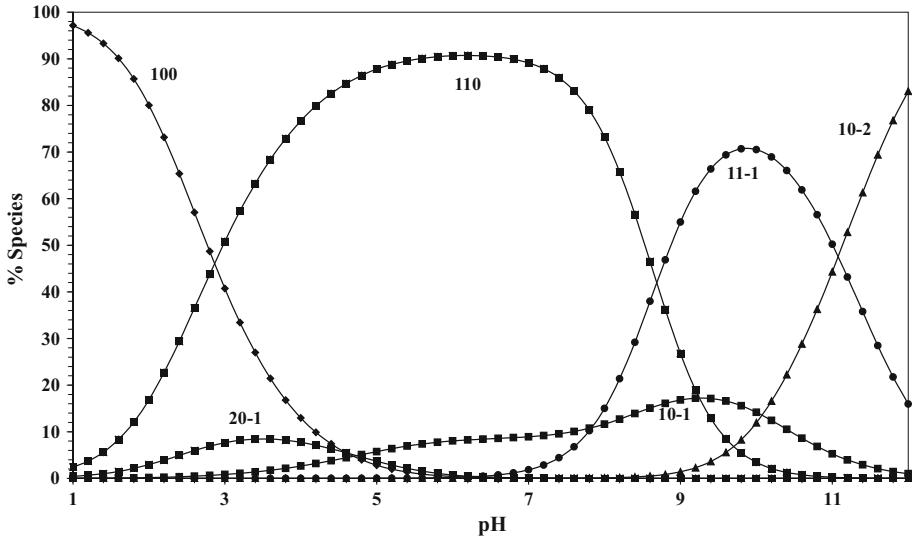

Fig. 1 Concentration distribution of various species as a function of pH in the Pd(MAMP)–glycylglycine system

the formation of a seven-membered chelate ring which is more strained and therefore less favored.

The distribution diagram for the Pd(MAMP)–glycylglycine system is given in Fig. 1. $[Pd(MAMP)L]^{+}$ (110) starts to form at lower pH, its concentration increases with increasing pH and reaches a maximum of 92% at pH = 5.8. A further increase in pH is accompanied by a decrease in the $[Pd(MAMP)L]^{+}$ concentration and an increase in the $[Pd(MAMP)LH_{-1}]$ (11–1) concentration, reaching a maximum of 87% at pH = 9.8, i.e., in the physiological pH range the deprotonated species (11–1) predominates.

For metal complexes with a series of structurally related ligands, a linear relationship holds between the logarithm of the stability constant of the complex and the logarithm of the acid dissociation constant of the ligand. The importance of these plots is that they afford a means of estimating the stabilities of metal complexes of closely related substances that have not yet been studied if their pK_a values are known. Figure 3S demonstrates a relationship between $\log_{10} \beta$ for the $[Pd(MAMP)(H_2O)_2]^{2+}$ complexes with peptides and their pK_a values.

Spectral bands of $[Pd(MAMP)(H_2O)_2]^{2+}$ and its glycyinamide complex are quite different in the position of the maximum wavelength and molar absorptivity. The spectrum of the $[Pd(MAMP)(H_2O)_2]^{2+}$ complex shows an absorption maximum at 289 nm. On the other hand, the spectrum obtained for [Pd(MAMP)(glycyinamide)] (110 species), mixture B, exhibits a band at 263 nm. The spectrum obtained for the [Pd(MAMP)(glycyinamide,H_{-1})] complex (11–1 species) (mixture C) exhibits a band at 255 nm. The progressive shift toward shorter wavelength in the absorption spectrum may be taken as evidence supporting the potentiometric measurements for the induced ionization of amide upon complex formation.

3.4 Complex Formation Equilibria Involving DNA Constituents

The pyrimidines: cytosine, uracil, uridine and thymine have only basic nitrogen donor atoms (N3-C4O group). Consequently the pyrimidines ligate in the deprotonated form through this site and they do not form protonated complexes. They form 1:1 and 1:2 complexes with $[Pd(MAMP)(H_2O)_2]^{2+}$. The thymine complex is more stable than that of uridine, most probably owing to the high basicity of the N3 group of thymine resulting from the extra electron donating methyl group. As a result of the high pK_a values of pyrimidines ($pK_a \approx 9$) and the fact that they are monodentates, the complexes are formed only above pH $\approx$ 6, supporting the view that the negatively charged nitrogen donors of pyrimidine bases are important binding sites in the neutral and slightly basic pH ranges.

Table 3 Protonation constants of some selected nucleoside and nucleotide bases and CBDCA and their formation constants with $[Pd(MAMP)(H_2O)_2]^{2+}$ at 25 °C and 0.1 mol·dm^{-3} ionic strength

System	l	p	r[a]	$\log_{10}\beta$[b]	S[c]
1,1-Cyclobutane dicarboxylic acid	0	1	1	5.62 (0.002)	1.6×10^{-8}
	0	1	2	8.66 (0.01)	
	1	1	0	7.20 (0.06)	8.6×10^{-7}
	1	1	1	11.35 (0.1)	
Uracil	0	1	1	9.28 (0.006)	2.42×10^{-8}
	1	1	0	9.13 (0.05)	2.82×10^{-7}
	1	2	0	15.51 (0.09)	
Uridine	0	1	1	9.01 (0.01)	1.10×10^{-7}
	1	1	0	9.19 (0.04)	4.36×10^{-7}
	1	2	0	13.04 (0.06)	
Thymine	0	1	1	9.58 (0.00)	8.14×10^{-8}
	1	1	0	10.07 (0.07)	8.33×10^{-7}
	1	2	0	13.93 (0.09)	
Cytosine	0	1	1	4.59 (0.04)	1.79×10^{-8}
	1	1	0	4.87 (0.08)	2.25×10^{-7}
	1	2	0	7.38 (0.07)	
Inosine	0	1	1	8.81 (0.006)	4.26×10^{-8}
	1	1	0	7.46 (0.1)	
	1	2	0	11.32 (0.1)	8.17×10^{-6}
	1	1	1	13.42 (0.06)	
Inosine 5′ − monophosphate	0	1	1	9.15 (0.006)	2.6×10^{-8}
	0	1	2	15.21 (0.01)	
	1	1	0	10.28 (0.07)	$1.67 \times 1^{0-8}$
	1	2	0	19.65 (0.07)	
	1	1	1	16.33 (0.08)	
	1	2	1	25.61 (0.07)	
	1	1	2	19.34 (0.08)	

[a] l, p and r are the stoichiometric coefficients corresponding to $Pd(MAMP)^{2+}$, nucleoside/nucleotide bases and H^+, respectively

[b] Standard deviations are given in parentheses

[c] Sum of square of residuals

Cytosine undergoes N3 protonation under mildly acidic conditions. The value obtained for its protonation constant is 4.59. The lower values of the stability constants of its complexes, listed in Table 3, reflect the difference in the basicity of the donor sites.

The purines, inosine and inosine 5′-monophosphate have two metal ion binding centers, the N1 and N7 nitrogens. The pH dependent binding of these N-donors has already been reported. Inosine may protonate at N7 forming a (N1H–N7H) monocation. In the present study, the pK_a of N1H was determined (pK_a = 8.81). The pK_a of N7H is 1.2 [38]. It was reported [39] that, in the acidic pH range, the metal ion is coordinated to N7, while N1 remained protonated. The results show that inosine forms the complexes 110 and 111. The species 111 is formed in the acidic pH region and it corresponds to a N7 coordinated complex, while the N1 nitrogen is in a protonated form. In inosine, the pK_a of the protonated form ($\log_{10} \beta_{111} - \log_{10} \beta_{110}$) is 5.96, which means that N1H is still protonated and is acidified by 2.85 pK units (8.81 – 5.96), Table 3. The lowering of the pK_a value of N1H upon coordination was reported previously [40]. Raising the pH could switch the coordination sites and result in a gradual change from N7 binding to N1 binding with an increase of pH as was suggested [39]. The monoprotonated 111 species reaches a maximum of 97% at pH = 3.6 (Fig. 2), which has the N7 site unprotonated and this is the potential coordination site at low pH. The binding site at the higher pH was disputed and a gradual change from N7-binding to N1-binding with an increase of pH was suggested [39]. Thus, 110 species prevails at pH = 6.2–7.8 while the 120 species reaches a maximum of 60% at pH = 9.0.

Inosine-5′-monophosphate (5′-IMP) forms a stronger complex with $[Pd(MAMP)(H_2O)_2]^{2+}$ than does inosine; the $\log_{10} \beta_{110}$ value is 10.28 compared to 7.46 for the inosine complex. The extra stabilization can be attributed to the triply negatively charged 5′-IMP^{3-}) ion. The results also show that IMP forms 110, 120, 111, 112 and 121 complexes (Table 3), i.e., the 5′-IMP complex has two protonated species associated with the 1:1 complex, namely 111 and 112, and their pK_a values are 6.05 and 3.01, respectively, with only one protonated species with 1:2 sroichiometry, namely 121. The species 112 was not detected with the Pd(aliphatic amines) complexes studied previously [41, 42]. This may be

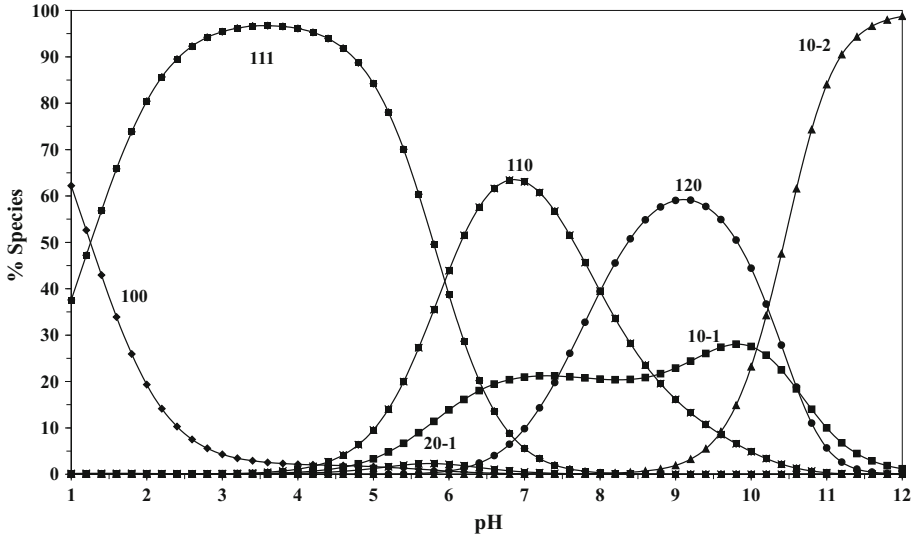

Fig. 2 Concentration distribution of various species as a function of pH in the Pd(MAMP)–inosine system

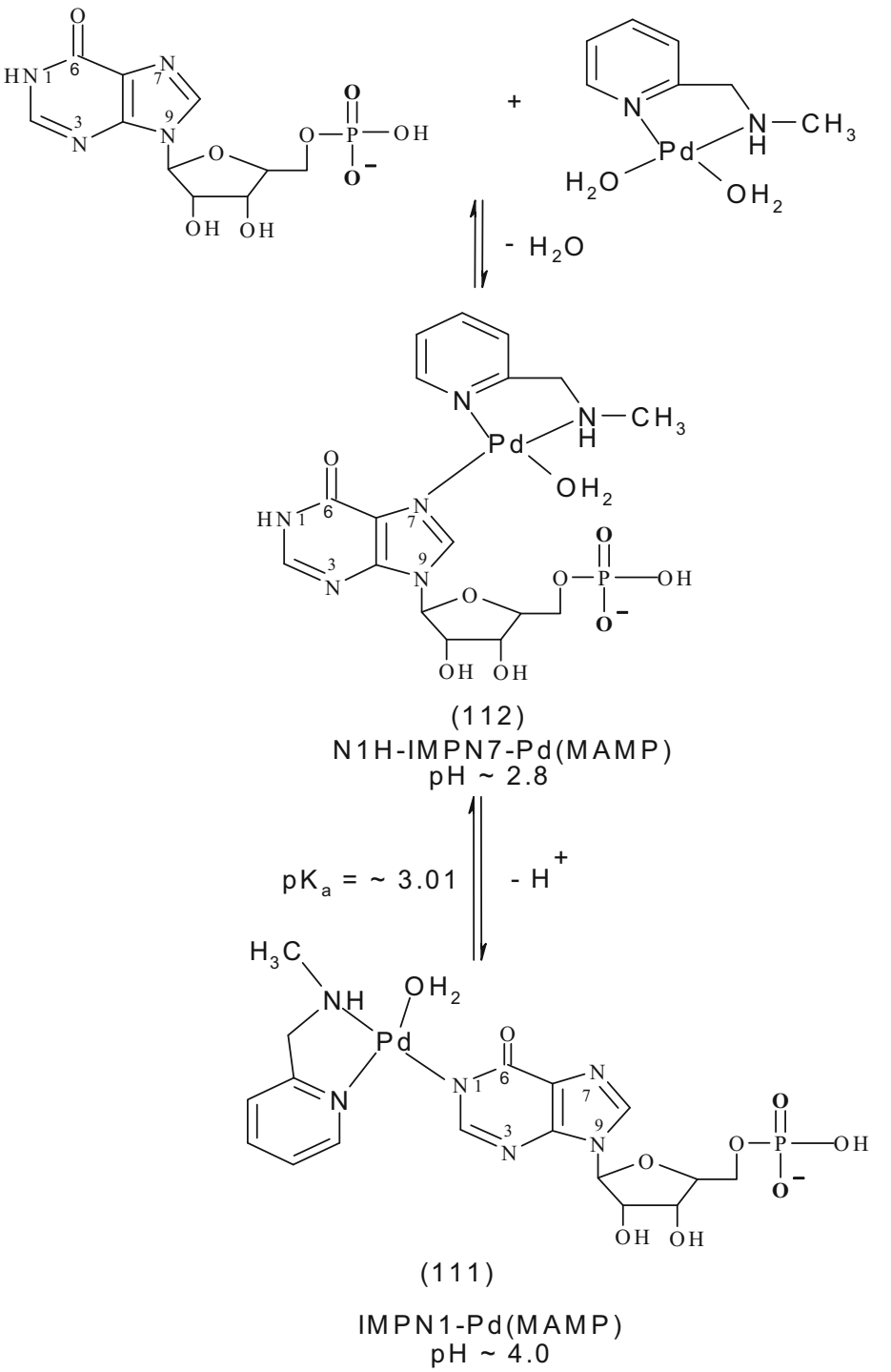

Scheme 4 Proposed coordination process of $Pd(MAMP)^{2+}$ with 5′-IMP

interpreted on the basis that the 112 is stabilized through back bonding to the π-system of the pyridine rings. In the fully protonated species (112), the two protons bound to N1 and the phosphate groups, exist at pH ∼ 2.8 or lower. The unprotonated N7 site in the diprotonated 112 species is the potential coordination site at low pH. In the (111) complex species, the single proton binds to the phosphate group.

The pK_a values of the protonated species of the IMP complex are 3.01 ($\log_{10} \beta_{112} - \log_{10} \beta_{111}$) and 6.05 ($\log_{10} \beta_{111} - \log_{10} \beta_{110}$). i.e., the stability constant difference (3.01) between the (112) and (111) complexes is due to the N1 deprotonation and the stability constant difference (6.05) between the (111) and (110) complexes is due to the $-PO_2(OH)$ group. The N1H group was acidified upon complex formation by 6.14 (9.15 − 3.01) pK units for IMP. Acidification of the N1H group upon complex formation is consistent with previous reports for IMP and GMP complexes [40]. The phosphate group was not acidified upon complex formation since it is far away from the coordination center [35]. A proposed coordination process of $Pd(MAMP)^{2+}$ with 5′-IMP is reported in Scheme 4.

The IMP complexes are more stable than those of the pyrimidines. The extra stabilization may be due to either the involvement of the phosphate group in hydrogen bonding with the exocyclic amine [43, 44], which will favor complex formation, or the different coulombic forces involved in the interaction of the trinegatively charged 5′-IMP ion and the mononegatively charged pyrimidinic ions with $Pd(MAMP)^{2+}$.

3.5 Ring Opening of [Pd(MAMP)(CBDCA)] and the Formation of [Pd(MAMP)(CBDCA-O)(DNA)]

The presence of ring-opened species was confirmed [45] using ^{1}H-NMR for cis-$[Pt(NH_3)_2(CBDCA\text{-}O)(5'\text{-}GMP\text{-}N7)]$. These studies indicate that CBDCA is attached through one carboxylate oxygen and 5′-GMP through N7 of the purine base. The ring-opened species was further confirmed by kinetic studies of the [Pd(diammine)(CBDCA)] complex and 5′-IMP. These studies conclude that CBDCA is attached through one carboxylate oxygen and 5′-GMP through N7 of the purine base. Also, such a reaction for [Pd(en)(CBDCA)] with thiourea, inosine 5′-monophosphate or iodide was mechanistically investigated [36]. It seems therefore to be of considerable interest to conduct an investigation in solution to prove the mechanism of the ring opening reaction of chelated CBDCA by DNA constituents. The potentiometric data for the system consisting of $[Pd(MAMP)(H_2O)_2]^{2+}$, CBDCA and some DNA constituents were fitted by assuming different models. The accepted model for pyrimidines is consistent with the formation of the 1110 species. The accepted model for IMP was found to consist of 1110 and 1111 species (Table 4). The proton on the N1H corresponds to pK_a of 5.90 (acidification of 9.15 – 5.90 = 3.25 pK units).

It is interesting to note that the quaternary complex of IMP is more stable than those of pyrimidines. This may be explained on the premise that the cyclobutane ring forms a close hydrophobic contact with the purine ring of IMP. Such hydrophobic contacts may contribute to the stabilization of the quaternary complexes. The same finding was obtained from an NMR investigation of the ring opening reaction of carboplatin with the 5′-GMP complex [36]. These studies conclude that CBDCA is attached through one carboxylate oxygen and 5′-IMP through N7 of the purine base. It should be recognized that further studies are necessary to elucidate the ring opening of chelated CBDCA by DNA constituents, especially multinuclear NMR measurements. These aspects will be considered in future investigations. Estimation of the concentration distribution of the various species in

Table 4 Formation constants for mixed ligand complexes of $[Pd(MAMP)(H_2O)_2]^{2+}$ with cyclobutanedicarboxylic acid and some DNA units at 25 °C and 0.1 mol·dm^{-3} ionic strength

System	*l*	*p*	*q*	*r*[a]	$\log_{10} \beta$[b]	S[c]
Uracil	1	1	1	0	17.70 (0.02)	1.1×10^{-6}
Thymine	1	1	1	0	17.97 (0.02)	8.0×10^{-7}
Cytosine	1	1	1	0	13.01 (0.02)	7.7×10^{-7}
Inosine	1	1	1	0	17.71 (0.03)	1.9×10^{-6}
Inosine-5′-monophosphate	1	1	1	0	18.65 (0.08)	1.1×10^{-9}
	1	1	1	1	24.55 (0.007)	

[a] *l*, *p*, *q* and *r* are the stoichiometric coefficients corresponding to $Pd(MAMP)^{2+}$, cyclobutanedicarboxylic acid, DNA subunits and H^+, respectively

[b] Standard deviations are given in parentheses

[c] Sum of square of residuals

solution provides a useful picture of metal ion binding. To illustrate the main features observed in the species distribution plots in these systems, the speciation diagram obtained for the Pd(MAMP)–CBDCA–IMP system is shown in Fig. 3. The quaternary species Pd(MAMP)–CBDCA–IMP species (1110) attains a maximum of 98% in the pH range 7.2–10.0. The quaternary protonated 1111 species reaches a maximum of 97% near pH = 3.9. This reveals that in the physiological pH range the ring opening of chelated CBDCA by DNA is quite feasible.

3.6 Displacement Reaction of Coordinated Inosine

It was shown above that N-donor ligands such as DNA constituents have an affinity for $[Pd(MAMP)(H_2O)_2]^{2+}$, which may have important biological implications since the

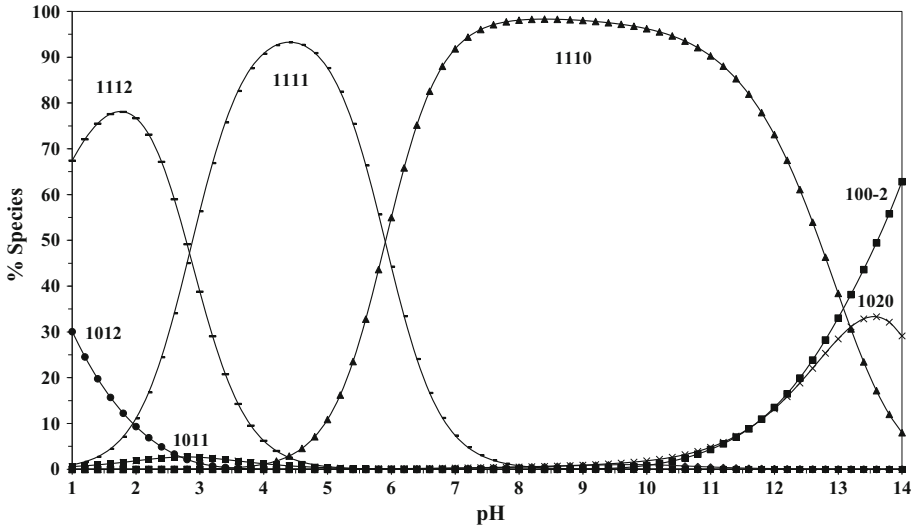

Fig. 3 Concentration distribution of various species as a function of pH in the Pd(MAMP)–CBDCA–IMP system

interaction with DNA is thought to be responsible for the antitumor activity of related complexes. However, the preference of $Pd^{(II)}$ to coordinate to S-donor ligands was previously documented [46, 47]. These results suggest that Pd(II)–N adducts can easily be converted into Pd–S adducts. Consequently, the equilibrium constant for such conversion is of biological significance, especially after the discovery of both $Pt^{(II)}$–methionine complexes in the urine of patients receiving cisplatin therapy and $Pt^{(II)}$–methionine complexes in blood plasma upon injection of cisplatin into rats [48].

If we consider inosine as a typical DNA constituent (presented by HL) and SMC as a typical S-ligand (presented by H_2B), the equilibria involved in the complex-formation and displacement reactions are:

$$HL \rightleftharpoons H^+ + L^-$$

$$H_2B \rightleftharpoons 2H^+ + B^{2-}$$

$$\underset{100}{[Pd(MAMP)]^{2+}} + L^- \rightleftharpoons \underset{110}{[Pd(MAMP)L]^+} \tag{8a}$$

$$\beta_{110}\left([Pd(MAMP)L]^+\right) = [Pd(MAMP)L]^+ \Big/ [Pd(MAMP)]^{2+}[L] \tag{8b}$$

$$\underset{100}{[Pd(MAMP)]^{2+}} + B^{2-} \rightleftharpoons \underset{110}{[Pd(MAMP)B]} \tag{9a}$$

$$\beta_{110}([Pd(MAMP)B]) = [Pd(MAMP)B] \Big/ [Pd(MAMP)]^{2+}\left[B^{2-}\right] \tag{9b}$$

$$\underset{100}{[Pd(MAMP)L]^+} + B^- \overset{K_{eq}}{\rightleftharpoons} \underset{110}{[Pd(MAMP)B]} + L^- \tag{10}$$

The equilibrium constant for the displacement reaction given in Eq. 10 is given by:

$$K_{eq} = [Pd(MAMP)B][L^-] \big/ [Pd(MAMP)L]^+\left[B^{2-}\right] \tag{11}$$

Substitution from Eqs. 8b and 9b in Eq. 11 results in:

$$K_{eq} = \beta_{110}([Pd(MAMP)B]) \big/ \beta_{110}\left([Pd(MAMP)L]^+\right) \tag{12}$$

$\log_{10} \beta_{110}$ values for the $[Pd(MAMP)L]^+$ and [Pd(MAMP)B] complexes are 7.46 and 9.63, respectively (Tables 1 and 3), and by substitution in Eq. 12 results in $\log_{10} K_{eq} = 2.17$. In case of using cytosine as a DNA constituent, $\log_{10} K_{eq} = 5.04$. Similarly, in the case of using methionine as a typical S-ligand and inosine as a typical DNA constituent, the $\log_{10}\beta_{110}$ values for the [Pd(MAMP)inosine] and [Pd(MAMP)methionine] complexes are 7.46 and 9.42, respectively (Tables 1 and 3), and hence the $\log_{10} K_{eq} = 1.96$. These values clearly indicate how sulfur ligands such as SMC and methionine are effective in displacing the DNA constituent, i.e., the main target in tumor chemotherapy. This in in agreement with the fact that simultaneous treatment with methionine and cisplatin reduces the cell toxicity of cisplatin [49].

Chelated cyclobutanedicarboxylate ($\log_{10} K = 7.20$, see Table 3) may undergo a displacement reaction with inosine. $\mathrm{Log}_{10} K_{eq}$ for such a reaction was calculated as described above and amounts to 0.24. In the case of the displacement reaction of coordinated cyclobutanedicarboxylate with cytosine, $\log_{10} K_{eq} = -2.59$. The low and negative values of the equilibrium constant for the displacement reaction of coordinated

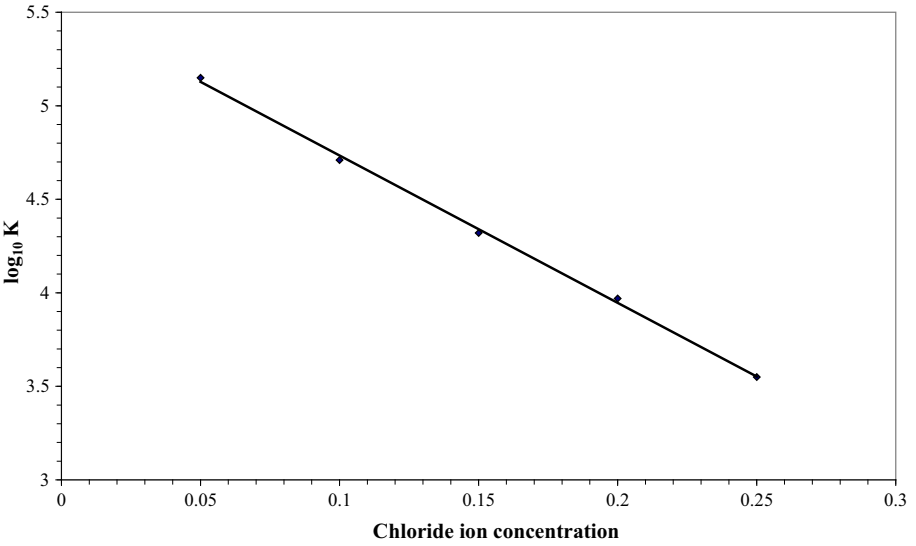

Fig. 4 Effect of chloride ion concentration on the stability of the Pd(BMAP–CBDCA) system where $\log_{10} K$ refers to the 110 species

cyclobutanedicarboxylate by a DNA constituent is of biological significance since it is in line with the finding that carboplatin interacts with DNA through ring opening of chelated CBDCA and not through displacement of CBDCA [36].

3.7 Effect of Chloride Ion Concentration on the Equilibrium Constants of $[Pd(MAMP)(H_2O)_2]^{2+}$ and Pd(MAMP)-CBDCA Complexes

Antitumor $Pt^{(II)}$–amine complexes are usually administrated as cis-dichloro-complexes. In human blood plasma the chloride content is high (100 mmol·dm^{-3}). Within many cells, the chloride ion concentration is much lower (only ca. 4 mmol·dm^{-3}). A realistic extrapolation of the present study to biologically relevant conditions will require information on the effect of the chloride concentration on the reported stability constants. The dichloro forms of antitumor Pt(II)–amine complexes persists in human blood plasma with its high 100 mmol·dm^{-3} Cl^- ion content [4]. Therefore, a realistic extrapolation of the present study to biologically relevant conditions will require information on the effect of the chloride concentration on the reported stability constants. The zero net charge on the complex hastens its passage through cell walls. Within many cells the Cl^- ion concentration is much lower, only 4 mmol·dm^{-3}. Under this low chloride ion concentration, the reactivity of the Pt(II)–amine complex increases. Chloride ion competes with OH^- for reaction with the $[Pd(MAMP)(H_2O)_2]^{2+}$ complex, so the pK_a values of the first and second coordinated water molecules increase with increasing chloride ion concentration as shown in the results given in Table 5. This means that hydrolysis is suppressed by increasing the chloride ion concentration. The data on the effect of chloride ion concentration on the hydrolysis constants of $[Pd(MAMP)(H_2O)_2]^{2+}$ and the stability of [Pd(MAMP)(CBDCA)] complex, keeping the ionic strength constant at 0.30 mol·dm^{-3}, are given in Tables 5 and 6, respectively. The stability constants of the Pd(MAMP)–CBDCA complexes, tend to decrease with increasing chloride ion concentration (Table 6). This can be accounted for

Table 5 Hydrolysis constants of $[Pd(MAMP)(H_2O)_2]^{2+}$ at different concentrations of chlorides at 25 °C and 0.3 mol·dm^{-3} ionic strength

[Cl$^-$]	l	p	r[a]	$\log_{10}\beta$[b]	pK_a[c]
0.0 mol·dm^{-3}	1	0	−1	−4.81 (0.02)	4.81
	1	0	−2	−14.96 (0.04)	10.15
	2	0	−1	−0.64 (0.08)	
0.05 mol·dm^{-3}	1	0	−1	−5.05 (0.03)	5.05
	1	0	−2	−15.28 (0.06)	10.23
	2	0	−1	−0.51 (0.09)	
0.1 mol·dm^{-3}	1	0	−1	−5.26 (0.06)	5.26
	1	0	−2	−15.56 (0.08)	10.30
	2	0	−1	−0.43 (0.1)	
0.15 mol·dm^{-3}	1	0	−1	−5.40 (0.07)	5.40
	1	0	−2	−15.85 (0.09)	10.45
	2	0	−1	−0.32 (0.1)	
0.20 mol·dm^{-3}	1	0	−1	−5.55 (0.03)	5.55
	1	0	−2	−16.14 (0.05)	10.59
	2	0	−1	−0.23 (0.09)	
0.25 mol·dm^{-3}	1	0	−1	−5.75 (0.03)	5.75
	1	0	−2	−16.49 (0.06)	10.74
	2	0	−1	−0.11 (0.08)	
0.3 mol·dm^{-3}	1	0	−1	−5.96 (0.03)	5.96
	1	0	−2	−16.87 (0.04)	10.91
	2	0	−1	−0.03 (0.07)	

[a] l, p and r are the stoichiometric coefficients corresponding to Pd(MAMP) $^{2+}$, ligand and H^+, respectively

[b] $\log_{10}\beta$ of $Pd(MAMP)^{2+}$

Standard deviations are given in parenthesis; sum of square of residuals are in the range 1–8 × 10^{-7}

[c] pKa_1 and pKa_2 of coordinated water molecules in $[Pd(MAMP)(H_2O)_2]^{+2}$

Table 6 Effect of chloride ion concentration on the formation constants of Pd(MAMP)-CBDCA at 25 °C and 0.3 mol·dm^{-3} (KCl + $NaNO_3$) ionic strength

[Cl$^-$] (mol.dm^{-3})	l	p	r[a]	$\log_{10}\beta$[b]	pK_a[c]
0.0	1	1	0	7.88 (0.09)	1.93
	1	1	1	9.81 (0.06)	
0.05	1	1	0	5.15 (0.08)	3.71
	1	1	1	8.86 (0.06)	
0.1	1	1	0	4.71 (0.07)	4.07
	1	1	1	8.78 (0.05)	
0.15	1	1	0	4.32 (0.08)	4.33
	1	1	1	8.65 (0.06)	
0.20	1	1	0	3.97 (0.09)	4.51
	1	1	1	8.48 (0.05)	
0.25	1	1	0	3.55 (0.07)	4.68
	1	1	1	8.23 (0.09)	
0.3	1	1	0	3.12 (0.05)	4.81
	1	1	1	7.93 (0.08)	

[a] l,p and r are the stoichiometric coefficients corresponding to $Pd(MAMP)^{2+}$, ligand and H^+, respectively

[b] $\log_{10}\beta$ of $Pd(MAMP)^{2+}$

Standard deviations are given in parenthesis; sum of square of residuals are in the range 3–8 × 10^{-7}

[c] pK_a of the protonated species (111) = $\log_{10}\beta_{111} - \log_{10}\beta_{110}$

on the basis that the concentrations of the active species, the mono- and the diaqua complexes, decrease with increasing [Cl^-]; this will in turn affect the stability of the complexes formed. A similar trend was observed for the reaction of $Pd(Me_4en)Cl_2$ (Me_4en = *N*,*N*,*Ń*,*Ń*-tetramethylethylenediamine) with inosine and 5′-inosine monophosphate as a function of the chloride concentration, where addition of Cl^- to the reaction mixture caused a significant decrease in the observed rate constants [42]. The variation in stability constant of the $Pd(MAMP)^{2+}$ complex with CBDCA, as a function of Cl^- ion concentration, is shown in Fig. 4. The pK_a of the protonated species 111 increases with increase of [Cl^-]. This may be explained on the premise that the chloride ion coordinated to $Pd^{(II)}$ ion stabilizes the uncoordinated carboxylic group proton through hydrogen bonding. This will lead to an increase of the pK_a value of the uncoordinated carboxylic group.

4 Quantum Chemical Calculations and Equilibrium Studies

Energy minimization studies were carried out on the basis of the semi-empirical PM3 level provided by HyperChem 7.5 software. The most stable structures for the metal$^{(II)}$ complexes obtained were subsequently optimized to the closest local minimum at the semiempirical level using PM3 parameterizations. The values of the following parameters: the highest occupied molecular orbital energy (E_{HOMO}), the lowest unoccupied molecular orbital energy (E_{LUMO}), the difference between HOMO and LUMO energy levels (ΔE), Mulliken electronegativity (χ), chemical potential (*Pi*), global hardness (η), global softness (*S*) and global electrophilicity (ω) [50–53] have been calculated [54] using this semi-empirical PM3 method as implemented in HyperChem [31]. In the first step, the molecular geometries of all compounds were fully optimized in the gas phase to gradients of 0.04 $kJ{\cdot}mol^{-1}{\cdot}Å^{-1}$ and afterwards the molecular descriptors were determined.

The concepts of the parameters χ and *Pi* are related to each other. The inverse of the global hardness is designated as the absolute softness σ.

To understand the mode of chelation and stability of these complexes in solution, we have optimized first the structure of metal complexes and then we have calculated and discussed the highest occupied molecular orbital–lowest unoccupied molecular orbital (HOMO–LUMO) gap for all these complexes (see Table 2S) in order to correlate the experimental results of stability constants with the calculated molecular parameters of the complexes (Table 7). The optimized structure for the [Pd–MAMP–α-Ala] complex as a representative example of the investigated compounds with the atomic numbering scheme is shown in the Fig. 5. The bond angles and bond lengths (Å) obtained from the energy minimum optimized structure of the [Pd–MAMP–α-Ala] complex are given. In

Table 7 Calculated E_{HOMO} (E_H), E_{LUMO} (E_L), energy band gap (ΔE), chemical potential (*Pi*), electronegativity (χ), electron affinity (*EA*), global hardness (η), absolute softness (σ), global softness (*S*) and electrophilicity index (ω) for the Pd-MAMP-L[a] complexes

Compound	HOMO[b]	LUMO[b]	ΔE	Pi[b]	EA[b]	χ	η	σ	S	ω
Pd-MAMP-α-Ala	−3.325	0.437	3.762	3.325	−0.44	1.444	1.88	0.532	0.266	0.554
Pd-MAMP-β-Ala	−3.090	0.550	3.640	3.090	−0.55	1.27	1.82	0.549	0.275	0.443

[a] *L* α-alanine, β-alanine

[b] The unit of HOMO, LUMO, Pi and EA is eV; 1ev = 1.6022×10^{-19} J

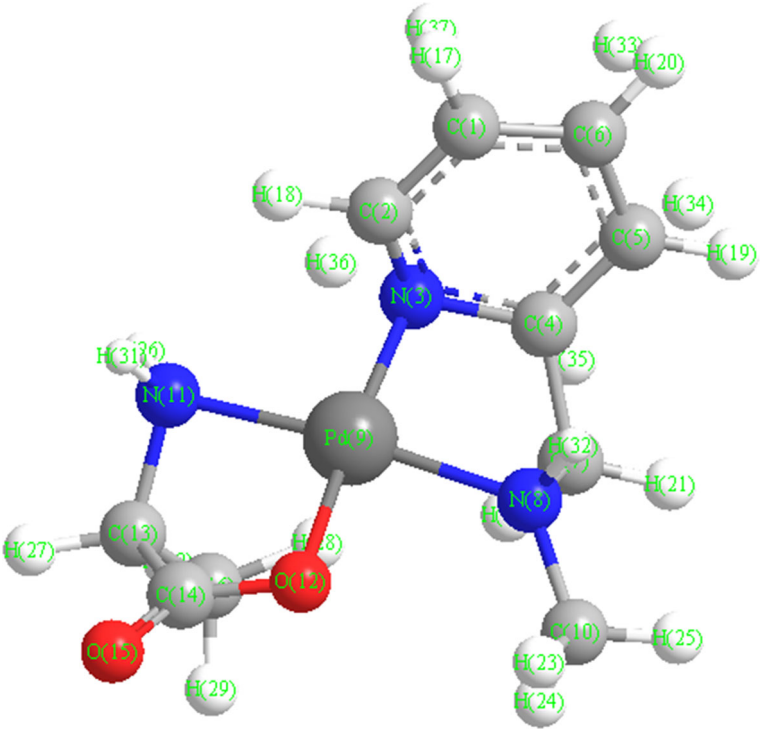

Fig. 5 The molecular structure of the [Pd(MAMP)–α-Ala] complex along with the atom numbering scheme

most of the cases, the actual bond lengths and bond angles are close to the optimal values, and thus the proposed structure of the compound is acceptable (See Table 3S).

The calculations for the molecular parameters support the experimental formation constant. The HOMO–LUMO gap is used as a direct indicator of stability [55, 56]. A large HOMO–LUMO gap indicates greater stability and decreased chemical reactivity. The results show the following trend in HOMO–LUMO gap for the complexes: Pd–MAMP–α-Ala > Pd–MAMP–β-Ala. The Pd–MAMP–α-Ala complex has an energy gap ($\Delta E = 3.762$) greater than that of the Pd–MAMP–β-Ala complex ($\Delta E = 3.640$). A large HOMO–LUMO gap is in accord with the experimental formation constant values.

According to the maximum hardness principle, greater hardness (η) causes more stability in the molecule [57]. Absolute hardness is half of the HOMO–LUMO energy gap. The hardness (η) calculated for the Pd(II) complexes is shown in Table 7. The hardness parameter of the complexes follows this sequence Pd–MAMP–α-Ala ($\eta = 1.88$) > Pd–MAMP–β-Ala ($\eta = 1.82$) which is also in accord with the energy gap and formation constants of the Pd(II) complexes.

5 Conclusions

The present investigation describes the formation equilibria of $[Pd(MAMP)(H_2O)_2]^{2+}$ with ligands of biological significance. In combination of stability constants data of such diaqua-complexes with amino acids, peptides and DNA constituents, it would be possible to

calculate the equilibrium distribution of the metal species in biological fluids where all types of ligands are present simultaneously. This would form a clear basis for understanding the mode of action of such metal species under physiological conditions. Amino acids form highly stable complexes, the substitutent on the α-carbon atom has a significant effect on the stability of the formed complex. Complex formation promotes deprotonation of the hydroxo group. The present study shows clearly that the $[Pd(MAMP)(H_2O)_2]^{2+}$ complex can form strong bonds with peptides and promote facile deprotonation of the peptide. In this work, it was possible to distinguish between the reactivity of nucleic bases, nucleosides and 5′-nucleotides. It is hoped that the obtained data from complex formation equilibria of $[Pd(MAMP)(H_2O)_2]$ with bioactive ligands in aqueous solution will be a significant contribution to workers carrying out mechanistic studies in biological media. The difference values between $\log_{10} K_1$ and $\log_{10} K_2$ for the interaction of $[Pd(MAMP)(H_2O)_2]$ with DNA constituents are positive, indicating that the coordination of the first ligand molecule to the metal ion is more favorable than the bonding to the second one. The molecular properties of the structures such as hardness and HOMO–LUMO energy gap supported the experimental formation constants of these complexes.

References

1. Rosenberg, B., Van Camp, L., Trasko, J.E., Mansour, V.H.: Platinum compounds: a new class of potent antitumour agent. Nature **222**, 385–386 (1969)
2. Wong, E., Giandomenico, C.M.: Current status of platinum-based antitumor drugs. Chem. Rev. **99**, 2451–2466 (1999)
3. Guo, Z., Sadler, P.J.: Medicinal inorganic chemistry. Adv. Inorg. Chem. **49**, 183–306 (2000)
4. Rosenberg, B.: In: Sigel, H. (ed.) Metal Ions in Biological Systems, vol. 11, pp. 127–196. Marcel Dekker, New York (1980)
5. Roberts, J.J.: In: Eichhorn, G.L., Marzilli, L.G. (eds.) Metal Ions in Genetic Information Transfer, vol. 11, pp. 273–332. Elsevier, Amsterdam (1981)
6. Gill, D.S.: In: Hacker, M.P., Douple, E.B. (eds.) Platinum Coordination Complexes in Cancer Chemotherapy, vol. 11, pp. 267–278. Nijhoff, Boston (1984)
7. Heim, M.E.: In: Keppler, B.K. (ed.) Metal Complexes in Cancer Chemotherapy, vol. 11, p. 9. VCH, Weinheim (1993)
8. Summa, N., Soldatović, T., Dahlenburg, L., Bugarčić, Ž.D., van Eldik, R.: Kinetics and mechanism of the substitution reactions of $[PtCl(bpma)]^+$, [PtCl(gly-met-S,N,N)] and their aqua analogues with L-methionine, glutathione and 5‘-GMP. J. Biol. Inorg. Chem. **12**, 1141–1150 (2007)
9. Bugarčić, Ž.D., Nandibewoor, S.T., Hamza, M.S.A., Heinemann, F., Van Eldik, R.: Kinetics and mechanism of the reactions of Pd(II) complexes with azoles and diazines. Crystal structure of $[Pd(bpma)(H_2O)](ClO_4)_2{\cdot}2H_2O$. Dalton Trans. **24**, 2984–2990 (2006)
10. Lippert, B. (ed.): Cisplatin Chemistry and Biochemistry of Leading Anticancer Drugs. Wiley-VCH, Zürich (1999)
11. Wang, D., Lippard, S.J.: Cellular processing of platinum anticancer drugs. Nat. Rev. Drug Discov. **4**, 307–320 (2005)
12. Abd El-Karim, A.T., El-Sherif, A.A.: Potentiometric, thermodynamics and coordination properties for binary and mixed ligand complexes of copper(II) with imidazole-4-acetic acid and tryptophan or phenylalanine aromatic amino acids. J. Solution Chem. **45**, 712–731 (2016)
13. Abdelkarim, A.T., Al-Shomrani, M.M., Rayan, A.M., El-Sherif, A.A.: Mixed ligand complex formation of cetirizine drug with bivalent transition metal(II) ions in the presence of 2-aminomethylbenzimidazole: synthesis, structural, biological, pH-metric and thermodynamic studies. J. Solution Chem. **44**, 1673–1704 (2015)
14. Rayan, A.M., Abdlkarim, A.T., Ahmed, M.M., El-Sherif, A.A., Barakat, M.H.: Complex formation of cetirizine drug with bivalent transition metal(II) ions in the presence of alanine: synthesis, characterization, equilibrium studies, and biological activity studies. J. Coord. Chem. **68**, 678–703 (2015)

15. Abdelkarim, A.T., El-Sherif, A.A.: Physicochemical studies and biological activity of mixed ligand complexes involving bivalent transition metals with a novel Schiff base and glycine as a representative amino acid. J. Eur. Chem. **5**, 328–333 (2014)
16. Aljahdali, M.S., Abdelkarim, A.T., El-Sherif, A.A., Ahmed, M.M.: Synthesis, characterization, equilibrium studies, and biological activity of complexes involving copper(II), 2-aminomethylthiophenyl-4-bromosalicylaldehyde Schiff base, and selected amino acids. J. Coord. Chem. **67**, 870–890 (2014)
17. Aljahdali, M., El-Sherif, A.A., Shoukry, M.M., Hosny, W.M., Abd-Elmoghny, M.G.: Complex formation equilibria of unusual seven coordinate Fe(III) complexes with DNA constituents. J. Solution Chem. **42**, 1663–1679 (2013)
18. El-Sherif, A.A., Shoukry, M.M., Abd-Elgawad, M.M.A.: Protonation equilibria of some selected α-amino acids in DMSO–water mixture and their Cu(II)-complexes. J. Solution Chem. **42**, 412–427 (2013)
19. El-Sherif, A.A., Shoukry, M.M.: The palladium(II)-picolylamine promoted hydrolysis of amino acid esters; kinetic evidence for inter- and intramolecular mechanisms. J. Progr. React. Kinet. Mech **36**, 215–226 (2011)
20. El-Sherif, A.A.: Synthesis and characterization of some potential antitumor palladium(II) complexes of 2-aminomethylbenzimidazole and amino acids. J. Coord. Chem. **64**, 2035–2055 (2011)
21. El-Sherif, A.A., Shoukry, M.M., El-Bahnasawy, R.M., Ahmed, D.M.: Complex formation reactions of palladium(II)-1,3-diaminopropane with various biologically relevant ligands. Kinetics of hydrolysis of glycine methyl ester through complex formation. Cent. Eur. J. Chem. **8**, 919–927 (2010)
22. Rau, T., Van Eldik, R.: In: Sigel, A., Sigel, H. (eds.) Metal Ions in Biological Systems, p. 340. Marcel Dekker, New York (1996)
23. Shoukry, M.M., Shehata, M.R., Abdel-Razik, A., Abdel-Karim, A.T.: Equilibrium studies of mixed ligand complexes involving (1,2-diaminopropane)-palladium(II) and some bioligands. Monatsh. Chem. **130**, 409–423 (1999)
24. El-Sherif, A.A., Shoukry, M.M., van Eldik, R.: Complex-formation reactions and stability constants for mixed–ligand complexes of diaqua(2-picolylamine)palladium(II) with some bio-relevant ligands. J. Chem. Soc., Dalton Trans. **7**, 1425–1432 (2003)
25. Rau, T., Shoukry, M.M., van Eldik, R.: Complex formation and ligand substitution reactions of (2-picolylamine)palladium(II) with various biologically relevant ligands. Characterization of (2-picolylamine)(1,1-cyclobutanedicarboxylato)palladium(II). Inorg. Chem. **36**, 1454–1463 (1997)
26. Mohamed, M.M.A., Shoukry, M.M.: Complex formation reactions of (N,N′-dimethylethylenediamine) palladium(II) with various biologically relevant ligands. Polyhedron **20**, 343–352 (2001)
27. Bates, R.G.: Determination of pH-Theory and Practice, 2nd edn. Wiley, New York (1975)
28. Stark, J.G., Wallace, H.G. (eds.): Chemistry Data Book, p. 75. Murray, London (1975)
29. Gans, P., Sabatini, A., Vacca, A.: An improved computer program for the computation of formation constants from potentiometric data. Inorg. Chim. Acta **18**, 237–239 (1976)
30. Pettit, L.: University of Leeds, Personal Communication
31. HyperChem version 7.5. Hypercube, Inc. (2003)
32. Perrin, D.D.: Stability Constants of Metal-Ion Complexes: Part B Organic Ligands. Pergamon Press, Oxford (1979)
33. Shehata, M.R.: Mixed ligand complexes of diaquo(2,2′-bipyridine)palladium(II) with cyclobutane-1,1-dicarboxylic acid and DNA constituents. Trans. Met. Chem. **26**, 198–204 (2001)
34. Lim, M.C.: Mixed–ligand complexes of palladium. Diaqua(ethylenediamine)palladium(II) complexes of ethanolamine, L-serine, L-threonine, L-homoserine, and L-hydroxyproline. Inorg. Chem. **20**, 1377–1379 (1981)
35. El-Sherif, A.A.: Coordination chemistry of palladium(II) ternary complexes with relevant biomolecules. In: Stoichiometry and Research, The Importance of Quantity in Biomedicine, pp. 79–120. In-Tech Publisher, Rijeka (2012)
36. Shehata, M.R., Shoukry, M.M., Nasr, F.M.H., van Eldik, R.: Complex-formation reactions of dichoroloro(S-methyl-L-cysteine) palladium(II) with bio-relevant ligands. Labilization induced by S-donor chelates. Dalton Trans. **6**, 779–786 (2008)
37. Lim, M.C.: Mixed-ligand complexes of palladium(II). Part 1. Diaqua(ethylenediamine)palladium(II) complexes of glycylglycine and glycinamide. J. Chem. Soc., Dalton Trans. **1**, 15–17 (1977)
38. Martin, R.B.: Nucleoside sites for transition metal ion binding. Acc. Chem Res. **18**, 32–38 (1985)
39. Maskos, K.: Spectroscopic studies on the copper(II)–inosine system. J. Inorg Biochem. **25**, 1–14 (1985)
40. Sigel, H., Massoud, S.S., Corfu, N.A.: Comparison of the extent of macrochelate formation in complexes of divalent metal ions with guanosine (GMP^{2-}), inosine (IMP^{2-}), and adenosine 5'-monophosphate (AMP^{2-}). The crucial role of N-7 basicity in metal ion–nucleic base recognition. J. Am. Chem. Soc. **116**, 2958–2971 (1994)

41. Shoukry, M.M., van Eldik, R.: Correlation between kinetic and thermodynamic complex-formation constants for the interaction of bis(amine)palladium(II) with inosine, inosine 5′-monophosphate and guanosine 5′-monophosphate. J. Chem. Soc., Dalton Trans. **13**, 2673–2678 (1996)
42. Shoukry, M.M., Hohmann, H., van Eldik, R.: Mechanistic information on the reaction of model palladium(II) complexes with purine nucleosides and 5′-nucleotides in reference to the antitumor activity of related platinum complexes. Inorg. Chim. Acta **198**, 187–192 (1992)
43. Ano, S.O., Intini, F.P., Natile, G., Marzilli, L.G.: Viewing early stages of guanine nucleotide attack on Pt(II) complexes designed with in-plane bulk to trap initial adducts. Relevance to cis-type Pt(II) anticancer drugs. J. Am. Chem. Soc. **119**, 8570–8571 (1977)
44. Kiser, D., Intini, F.P., Xu, Y., Natile, G., Marzilli, L.G.: Atropisomerization of cis-bis(5'GMP)–platinum(II)–diamine complexes with non-C2-symmetrical asymmetric diamine ligands containing NH groups directed to one side of the coordination plane. Inorg. Chem. **33**, 4149–4158 (1994)
45. Frey, U., Ranford, J.D., Sadler, P.J.: Ring-opening reactions of the anticancer drug carboplatin: NMR characterization of cis-[Pt(NH_3)$_2$(CBDCA-O)(5'-GMP-N7)] in solution. Inorg Chem. **32**, 1333–1340 (1993)
46. Rau, T., Alsfasser, R., Zahl, A., Van Eldik, R.: Structural and kinetic studies on the formation of platinum(II) and palladium(II) complexes with l-cysteine-derived ligands. Inorg. Chem. **37**, 4223–4230 (1998)
47. Lemma, K., Elmroth, S.K.C., Elding, L.I.: Substitution reactions of $[Pt(dien)Cl]^+$, $[Pt(dien)(GSMe)]^{2+}$, cis-[$PtCl_2(NH_3)_2$] and cis-$[Pt(NH_3)_2(GSMe)_2]^{2+}$ (GSMe = S-methylglutathione) with some sulfur-bonding chemoprotective agents. J. Chem. Soc., Dalton Trans. **7**, 1281–1286 (2002)
48. Provosta, K., Bouvet-Mullera, D., Crauste-Manciet, S., Moscovicia, J., Olivid, L., Vlaicd, G., Michalowicza, A.: EXAFS structural study of platinum-based anticancer drugs degradation in presence of sulfur nucleophilic species. Biochimie **91**, 1301–1306 (2009)
49. Alden, W.W., Repta, A.J.: Exacerbation of cisplatin-induced nephrotoxicity by methionine. Chem. Biol. Interact. **48**, 121–124 (1984)
50. Pearson, R.G.: Absolute electronegativity and hardness: applications to organic chemistry. J. Org. Chem. **54**, 1423–1430 (1989)
51. Geerlings, P., De Proft, F., Langenaeker, W.: Conceptual density functional theory. Chem. Rev. **103**, 1793–1874 (2003)
52. Parr, R.G.: Electrophilicity index. J. Am. Chem. Soc. **121**, 1922–1924 (1999)
53. Chattaraj, P.K., Giri, S.: Stability, reactivity, and aromaticity of compounds of a multivalent superatom. J. Phys. Chem. A **111**, 11116–11121 (2007)
54. Speie, G., Csihony, J., Whalen, A.M., Pie-Pont, C.G.: Studies on aerobic reactions of ammonia/3,5-ditert-butylcatechol Schiff-base condensation products with copper, copper(I), and copper(II). Strong copper(II)-radical ferromagnetic exchange and observations on a unique N-N coupling reaction. Inorg. Chem. **35**, 3519–3535 (1996)
55. Aihara, J.: Reduced HOMO–LUMO gap as an index of kinetic stability for polycyclic aromatic hydrocarbons. J. Phys. Chem. A **103**, 7487–7495 (1999)
56. Haddon, R.C., Fukunaga, T.: Absolute hardness as a measure of aromaticity. Tetrahedron Lett. **29**, 4843–4846 (1988)
57. Parr, R.G., Chattara, P.K.: Principle of maximum hardness. J. Am. Chem. Soc. **113**, 1854–1855 (1991)